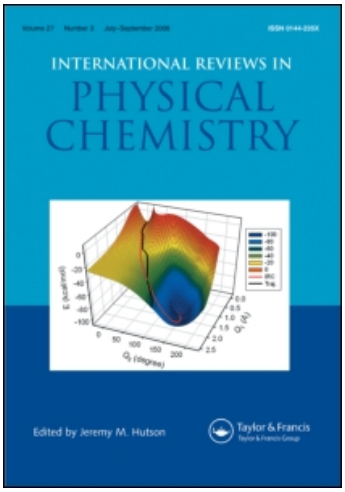

International Reviews in Physical Chemistry
Publication details, including instructions for authors and subscription information:
http://www.informaworld.com/smpp/title~content=t713724383

Light scattering in the study of colloidal and macromolecular systems

P. Johnson[a]
[a] Cavendish Laboratory, Cambridge, England

To cite this Article Johnson, P.(1993) 'Light scattering in the study of colloidal and macromolecular systems', International Reviews in Physical Chemistry, 12: 1, 61 — 87
To link to this Article: DOI: 10.1080/01442359309353278
URL: http://dx.doi.org/10.1080/01442359309353278

INTERNATIONAL REVIEWS IN PHYSICAL CHEMISTRY, 1993, VOL. 12, NO. 1, 61–87

Light scattering in the study of colloidal and macromolecular systems

by P. JOHNSON
Cavendish Laboratory, Madingley Road,
Cambridge CB3 0HE, England

The fundamentals of the traditional (integrated) light scattering method are reviewed together with the application to a variety of macromolecules of both corpuscular and asymmetric form. Brief mention is made of the application of optical methods to the investigation of particles comparable and larger than the wavelength of the light and of much higher refractive index. Usually termed Mie theory, this involves complex calculations which, in modern instruments, are performed by built-in computers. For much larger particles, Fraunhofer diffraction is available, which can be applied for particle dimensions up to 700 μm. With the introduction of the laser, improvements in traditional light scattering became possible but more importantly, new possibilities arose which made use, particularly, of the coherence properties of laser radiation. Thus dynamic light scattering is concerned with the intensity fluctuations in time which arise from the various possible motions of the scattering particles. Special digital correlators have been introduced to measure the intensity correlation function as the delay time is varied over a large range of values. For spherical particles in dilute solution this gives accurate translational diffusion coefficients and a semi-quantitative measure of the polydispersity for a wide range of particle sizes (from enzymes to viruses). For rod-like particles, in favourable cases, a rotational diffusion coefficient may also be determined and in the case of flexible chain-like molecules, information on the lower order internal modes of vibration may be obtained. For motile micro-organisms, new features on the correlation decay yield a measure of their velocity distribution. All these fields are in active development.

1. Traditional light scattering

1.1 *Scattering in gaseous systems*

An interest in light scattering began more than 100 years ago (e.g. see Kerker (1969)) but the quantitative side of its study may be said to have begun with the work of Lord Rayleigh (Third Baron) (1871), probably inspired by the experiments of Tyndall (of the Tyndall cone). Rayleigh first treated the scattering of gases in terms of the old elastic solid theory of light, but later (1881) showed that the same results could be deduced from the electromagnetic theory of light. Assuming the scattering molecules to be small (cf λ) isotropic spheres in chaotic motion, the oscillating electric field of the light induced in them oscillating dipoles in the same direction. These were responsible for the scattered radiation. Since, in a dilute gas, the scattering centres are randomly positioned, intensities could be summed leading to the well-known equation:

$$i_\theta r^2/I_0 = \frac{8\pi^4\alpha^2 v}{\lambda_0^4}(1+\cos^2\theta), \tag{1}$$

where i_θ is the scattered intensity at a distance r from unit scattering volume (/ml) containing v particles, I_0 is the incident intensity, λ_0 is the wavelength in vacuo, α is the

0144-235X/93 $10·00

polarizability and θ is the angle between the incident and scattering directions. For practical purposes, where no absorption of the light occurs, α is replaced by an expression involving only the refractive index (r.i.) n of the scattering particles, i.e.

$$\alpha = \frac{n^2-1}{4\pi v} \approx \frac{n-1}{2\pi v}. \tag{2}$$

From (1) and (2), it follows that

$$i_\theta r^2/I_0 = \frac{2\pi^2(n-1)^2}{\lambda_0^4}\frac{1}{v}(1+\cos^2\theta). \tag{3}$$

The left-hand side (l.h.s.) of this equation is usually known as Rayleigh's ratio, R_θ and, providing calibration procedures are adequate (see Appendix A), can be evaluated in absolute terms. v, the number of scattering particles /ml can thus be derived since the other quantities appearing on the right-hand side (r.h.s.) are usually readily available. Further, since the weight concentration, c, (g/ml) may be written as vM/N_0, it follows that the molecular weight (M) may be determined if Avogadro's number (N_0) is assumed. Alternatively, as was performed by earlier workers, if M is assumed then the Avogadro number, N_0, may be obtained.

Although it was soon realized that Rayleigh's theoretical work went far towards explaining the blue colour of the sky and the general properties of natural light, experimental proof of its more quantitative aspects had to await the development of more sophisticated techniques, particularly for the complete removal of dust from gases and for the avoidance of stray light. This was performed by Cabannes (1915) and, later, by the next Lord Rayleigh (Fourth Baron), 1918, who performed careful measurements on dust-free air and other gases. In the following years detailed work on the scattered intensity and the state of polarization of the scattered light was performed, in which Raman and other Indian workers played a prominent part. Thus Raman and Ramanathan (1923a) studying the scattering of those vapours and gases which did not obey Boyle's Law, concluded that Rayleigh's law of scattering did not apply owing to the non-random distribution of the molecules. However using the Boltzmann distribution they were able to predict the magnitude of the deviations and showed that they were in agreement with those calculated from the Einstein–Smoluchowski fluctuation theory. The same authors (1923b) proceeded to evaluate the Avogadro number from the scattering by pure distilled water using the Einstein–Smoluchowski expression.

1.2. *Scattering in liquids and solutions*

Turning now to the scattering by liquids and liquid solutions, the much closer proximity and greater ordering of the molecules makes for very serious differences from gaseous scattering. These differences were in fact readily observed and in general the scattering from the liquid state is much weaker (approximately fiftyfold) than that from an equivalent mass of the vapour state. This arises from the destructive interference of light scattered by different but partially ordered molecules. If the ordering is made more complete, then the scattering becomes even smaller and theoretically zero in the case of a perfect crystal. Smoluchowski (1908) treated the scattering from a pure liquid in terms of the 'fluctuations' occurring (from perfect order) in density which, in turn, gave rise to changes in dielectric constant and refractive index. Einstein (1910) extended these ideas to two-component liquids, each consisting of isotropic molecules whose dimensions

were small compared with the wavelength. Fluctuations could now occur not only in the density but also in the concentration of one component with respect to the other. For the systems of relevance here one component (the solvent) is usually present in great excess, the macromolecular or colloidal solute usually being present at a concentration less than 1 g/100 ml. Under such circumstances the excess scattering of solution over the pure solvent may be related to the concentration fluctuations occurring and this led directly to the fundamental equation of light scattering,

$$Kc/R_{90}=\frac{1}{M}+2Bc,$$

where

$$K=2\pi^2 n_0^2(\mathrm{d}n/\mathrm{d}c)^2/N_0\lambda_0^4. \tag{4}$$

n_0 is the refractive index of the solvent and B is the coefficient of the concentration term (often termed the second Virial coefficient) relating osmotic pressure (π) to concentration:

$$\pi/cRT=\frac{1}{M}+Bc. \tag{5}$$

Here R is the gas constant and T the absolute temperature. B is known to reflect excluded volume effects as well as the occurrence of intermolecular forces between solute molecules. It is of interest that if the polarizability α in equation (2) had been written as $(n^2-n_0^2)/4\pi v$, then providing n (the refractive index of the particles) is not very different from n_0 (the r.i. of the solvent) an equation similar to equation (4) is obtained but without the term, $2Bc$. In certain cases, this term may be ignored but in general its presence is accepted. Determination of molecular weight thus involves the determination of R_{90} over a range of concentration and extrapolation to infinite dilution. Where the solute is polydisperse, it may readily be shown (see Appendix B) that the weight-average value, M_w, is obtained (e.g. Doty and Edsall, (1951)).

1.3. *Scattering by particles with dimensions* $\leqslant\lambda$

Equation (4) is applicable only if the solute molecules are isotropic and small compared with the wavelength ($<\lambda/20$). For such materials the scattering molecules may be regarded as point sources. However when particle dimensions become comparable or greater than λ, this is no longer justifiable and an important consequence is that light scattered from different parts of the molecule is subject to phase differences at the detector and is thus involved in interference effects, particularly in directions for $\theta>90°$ (see figure 1 (*a*)). For situations in which the distortion of the electric field of the incident beam may be neglected (i.e. where the refractive index of the particle is not very different from that of the solvent), the total amplitude in a given direction is obtained by summing over all the volume elements of the particle. Debye (1915) had performed such calculations in connection with X-ray scattering and later (1947) extended these to include light scattering by flexible chain-like macromolecules. He thus derived for the ratio of the intensity at angle θ, $I(\theta)$, relative to that, $I(0)$ at 0° (or $P(\theta)$) the expression

$$P(\theta)=\frac{2}{x^2}[\exp(-x)-(1-x)], \tag{6}$$

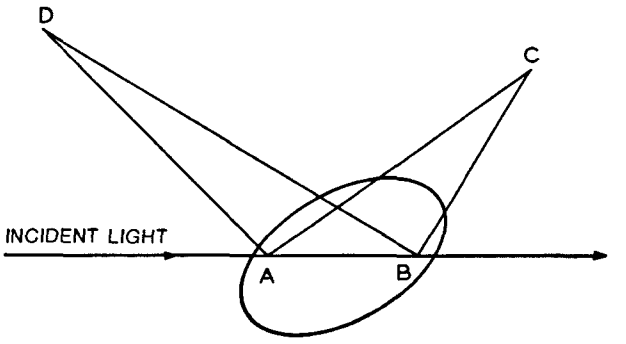

(*a*)

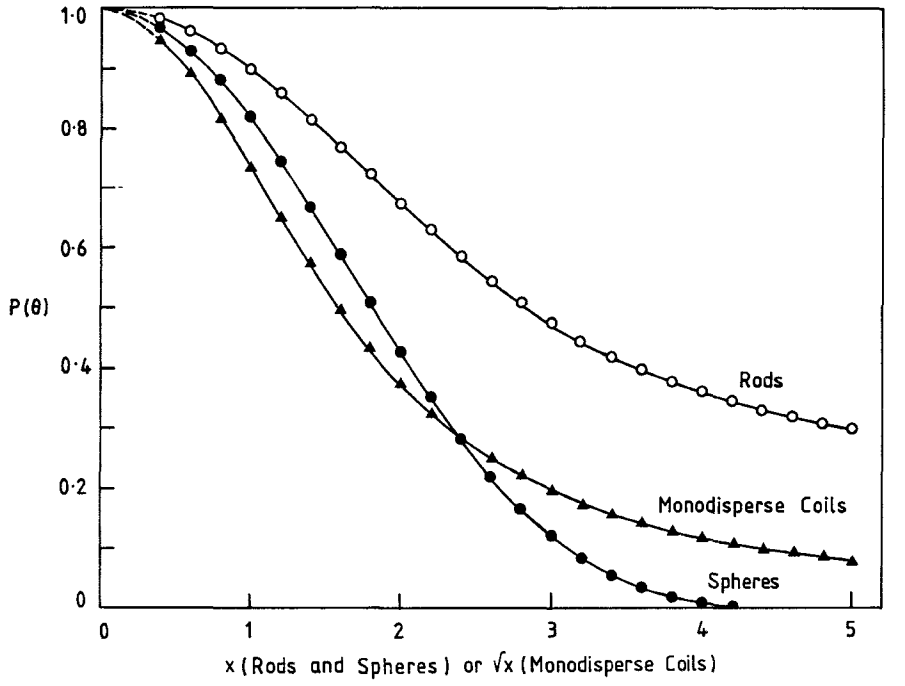

(*b*)

Figure 1. (*a*) Interference effects for particles whose dimensions are comparable with wavelength. Path difference (AB + BC − AC) is much smaller in the forward than the backward (AB + BD − AD) direction. (*b*) Plot of $P(\theta)$ against suitable function of molecular dimension for: Coils, $\sqrt{x} = ksR_g/\sqrt{6}$, R_g = radius of gyration, Rods, $x = ksL/2$, L = length of rod, Spheres, $x = ksD/2$, D = diameter.

where

$$x = k^2 s^2 \frac{R_{ee}^2}{6}, \qquad \text{with } k = \frac{2\pi}{\lambda}, \qquad s = 2\sin\theta/2 \tag{7}$$

and R_{ee}^2, the average square end to end distance of the polymer chain. Other workers carried out similar calculations for other models (e.g. rods, ellipsoids of revolution) thus obtaining the so-called particle scattering factor, $P(\theta)$, for each model. Figure 1 (*b*) demonstrates the dependence of $P(\theta)$ on x (or $\sqrt{x}$) which contains not only $\theta/2$ but also a characteristic dimension of the macromolecule (see Doty and Edsall, (1951)). In the general case Debye showed that $P(\theta)$ may be written

$$P(\theta) = 1 - \left(\frac{4\pi n_0}{\lambda_0}\sin\theta/2\right)^2 R_g^2/3 + \text{higher terms}, \tag{8}$$

where R_g is the radius of gyration defined by $(1/V)\int r^2 \mathrm{d}V$ (V being volume, with r being the distance from the centre of mass of the volume element $\mathrm{d}V$) and higher terms involve average fourth (and higher) powers of distances within the particle. Knowledge of the variation of $P(\theta)$ as a function of θ can thus give information about the dimensions of the scattering particles (see later). It should be stressed that such $P(\theta)$ factors are valid only where the particle refractive index is not too different from that of the solvent and its characteristic dimension (R) not too large compared with wavelength. These restrictions (often termed the Rayleigh–Gans limitations) are expressed quantitatively in the inequality,

$$\frac{4\pi R}{\lambda_0}(n - n_0) \ll 1. \tag{9}$$

If $P(\theta)$ deviates significantly from unity, it is clear that R_{90} in equation (4) must be corrected to the value it would have in the absence of interference effects, $R_{90}/P(90)$, and Zimm (1948) showed that under these circumstances equation (4) becomes (to a good approximation)

$$KcP(90)/R_{90} = \frac{1}{M} + 2BP(90)c. \tag{10}$$

$P(90)$ values may be obtained from measurements of the dissymmetry, z, $(= i_\theta / i_{180-\theta})$ through the various tabulations which are available (e.g. see Doty and Edsall (1951)). A plot of the l.h.s. of equation (10) against c thus gives $1/M$ as an intercept on the ordinate, with $2BP(_{90})$ as slope.

A more general method, using biaxial extrapolation, was proposed by Zimm (1948). Since interference effects disappear at 0°, extrapolation to 0° from measurements at a range of higher angles avoids the use of a correction factor and makes full use of angular data. Zimm suggested a plot of $Kc/R_\theta v \sin^2(\theta/2) + kc$, where k is an arbitrary constant whose function is to spread out the data conveniently. An example is shown in figure 2. Two sets of nearly parallel lines occur, one at constant angle and varying concentration (the more horizontal), and the other at constant concentration and varying angle (the steeper). The varying concentration plots are extrapolated to strike a vertical ordinate at the particular values of $\sin^2\theta/2$. The steeper plots are extrapolated to strike an ordinate set at kc. Thus two lines, corresponding to zero angle (with varying concentration) and zero concentration (with varying angle) respectively are obtained. On extrapolation these lines should intersect on the main ordinate axis to give $1/M$.

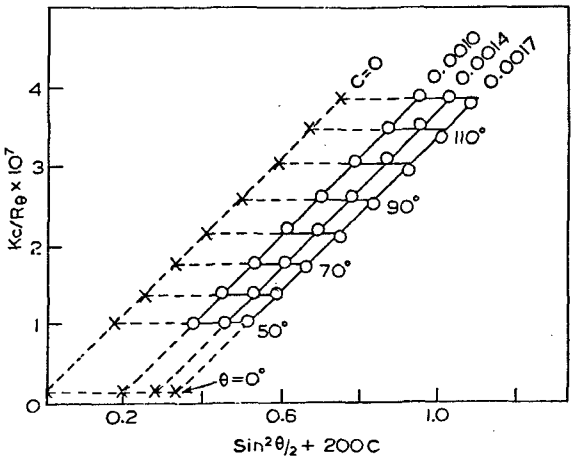

Figure 2. Zimm biaxial plot for toxin–antitoxin aggregate.

Zimm pointed out also that the variation of Kc/R_θ with angle contained essential information for determining the dimensions of the scattering particle. Thus it can be seen from equation (8) that

$$\frac{\text{Initial Slope of } c=0 \text{ line}}{\text{Intercept}} = \frac{16\pi^2 n_0^2}{3}\left(\frac{R_g}{\lambda_0}\right)^2, \tag{11}$$

where R_g is the radius of gyration of the particle. For polydisperse systems, the R_g value obtained would be a z average.

In certain circumstances, the zero concentration line may reach a limiting slope at high values, and extrapolation to the ordinate axis yields $1/M_N$, where M_N is the number-average (Benoit, Holtzer and Doty (1954)). Correspondingly the slope may yield a different average of the radius of gyration. However doubts have been expressed regarding the practical realisation of such high extrapolation.

Summing up, it may be said that where the Rayleigh–Gans limitations are obeyed, the Zimm method of biaxial extrapolation provides a very sound and complete utilisation of intensity measurements over a range of angles, giving an accurate molecular weight value and probably less accurate radius of gyration. If, however, the particle dimensions are less than $\lambda/20$, $P(\theta)$ will not deviate far from unity, and equation (4) with corrected R_{90} values gives satisfactory M_W values. Providing the solute refractive index does not deviate too far from that of the solvent (i.e. $n/n_0 \leqslant 1{\cdot}2$) an upper limit for the characteristic dimension is usually set at about 10^4 Å. For larger particles or those for which $n/n_0 > 1{\cdot}3$, the more complex Mie theory has to be applied.

1.4. *Scattering in general*

As yet two classes of scattering particles only have been considered:

(i) Rayleigh scatterers for which linear dimensions are much smaller than the wavelength of the light scattered ($< \lambda/20$), and whose internal structure makes them isotropic, and

(ii) Rayleigh-Gans particles for which equation (9) holds imposing conditions upon both particle dimensions and refractive index relative to the suspending solvent.

Undoubtedly these classes are important, covering many soluble synthetic and biological polymeric systems. However many materials possess n/n_0 values larger than acceptable by equation (9), many possess dimensions much greater than λ_0, and for others both factors together cause serious departures from equation (9). In addition many scattering materials (inorganic metals sols particularly) significantly absorb light, necessitating the introduction of complex refractive indices.

Theoretical attempts to treat scattering in general go back more than 100 years and these have been well summarized by Kerker (1969). Of particular note are the contributions by Lorenz (1898), Mie (1908), and Debye (1909). More recently, in a very comprehensive treatment, van de Hulst (1957) has considered spheres covering a range of sizes and refractive indices as well as more complex shapes, and has attempted to relate the various approximations applying over restricted ranges of particle properties. Figure 3, adapted from that of van de Hulst, illustrates these inter-relations. It will be observed that four labelled areas occur approximately centrally along the outside of the square and, for each of these, simplified (though different) methods of computation apply. Rayleigh and Rayleigh–Gans systems have already been described. Fraunhofer diffraction analysis (see below) is now routinely involved in commercially available equipment (e.g. Malvern, Coulter, Microtrac) and is capable of being applied to particles with linear dimensions up to 600 μ and as low as 0·1 μ. Total reflection involves high and often complex values of the refractive index. Whilst Mie theory can be applied to spheres of any refractive index, somewhat simpler methods are also available for many systems including perfect conductors as shown by van de Hulst (1957). In the various corner regions of figure 3, overlap of the larger areas mentioned above occurs and in any one such region the alternative approaches yield the same results.

The interior of the square, where n/n_0 and $2\pi R/\lambda_0$ take on higher values is the region where general Mie theory is extensively applied. This represents a fundamental application of the Maxwell electromagnetic equations, taking account of the refractive

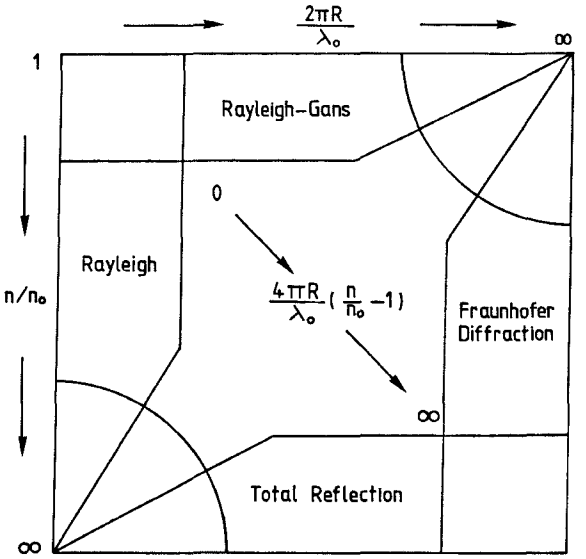

Figure 3. The different regimes of light scattering (adapted from van de Hulst (1957)).

indices (including complex values) of the solvent and spherical particle and the dimensions of the latter. In reaching the equations for scattering, the boundary conditions at the particle–solvent interface are applied, involving assumptions of the continuity of the normal components of the dielectric displacement and magnetic induction and the tangential components of the electric and magnetic field. These equations are quite complex involving spherical Bessel functions and Legendre polynomials. However, several authors have utilised them numerically by computer (see Kerker (1969) for a listing) on spheres over a range of relative refractive indices and particle radii (in terms of $2\pi R/\lambda$) for angles ranging from $\theta = 0°$ to 180° (5° intervals). Thus Pangonis and Heller (1960) list respectively the intensities of the components with electric vectors perpendicular and parallel to the scattering plane as well as the total intensity under the above conditions. Undoubtedly such tabulations have proved very useful but van der Hulst (1957), in particular has drawn attention to the dangers of interpolation where rapidly varying effects arise from slight changes in the varying parameters. With the advent of the modern computer with its ability to process numerical data rapidly, such interpolation can now be avoided as well as the need to consult tables. The computations, using the actual experimental parameters of the particular system being studied may be performed *ab initio* using programs which themselves contain the elements of Mie theory.

Mie (1908) made his calculations on the basis of monodisperse spheres of homogeneous structure, but several workers have pointed out the relevance, particularly amongst biological cells, of structured (or often coated) cells, in which the refractive index is not constant throughout. Thus Aden and Kerker (1951) and later Brunsting and Mullaney (1972) worked out the theory of such structures and made comparisons with real systems. Progress on cylindrical models has also been reported by van de Hulst (1957) and Kerker (1969), but the reader is directed to these references for further information. Whilst such models and further refinements introduce extra theoretical complication, it seems likely that computer power will undoubtedly make their widespread application possible in the near future.

1.5. *Fraunhofer diffraction analysis*

This subject should strictly be considered under diffraction rather than scattering, but since the particle size range covered complements the Mie range so conveniently, it is useful to consider the two approaches together. An apparatus of the type shown in figure 4 is used. Light from a low power (e.g. 2 mw) He–Ne laser is expanded to produce a parallel beam (of diameter up to 2 cm) which falls upon a suspension of the test particles in a parallel sided glass cell. A lens, often called the Fourier lens, picks up light passing through the cell and brings it to a focus on a screen possessing an array of photo sensitive detecting elements. Light which passes undeviated through the cell is focused at the centre of the screen. Light diffracted by the suspended particles is deviated through an angle inversely proportional to the diameter of the assumed spherical particles and therefore for a monodisperse material appears with a maximum as a well-defined concentric ring on the detecting screen. For such a distribution, weaker concentric maxima occur at higher distances from the centre of the pattern (see e.g. Hecht (1987)). Particles of differing diameter produce maxima at different positions and the intensity distribution on the screen is a superposition of all the maxima and is therefore dependent on the size distribution of the suspended particles. The pattern observed on the screen is indeed the Fourier transform of the plane containing the

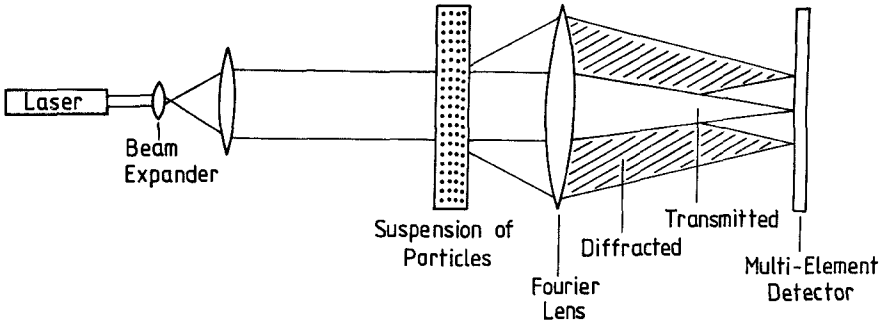

Figure 4. Apparatus for Fraunhofer particle size analysis.

diffracting particles. It should be emphasised that neither the precise position of the particles in the cell nor their motion suspension affect the position of their contribution to the overall pattern. The multi-element detector is able to assess the distribution of energy across the screen and thus to estimate the distribution of particle size in the suspension (see Swithinbank, Beer, Taylor and McCreath, 1977) for a discussion of the basic diffraction theory). In modern instruments the data from the detector is processed by computer so that a size distribution curve is produced in minutes. The lower size limit is approximately the wavelength of the light used and the upper limit is partly determined by the need to keep the particles in suspension. In the case of aerosols, which can be examined by this method, particles are kept suspended in a current of air.

When the various optical methods (Rayleigh, Rayleigh–Gans, Mie, and Fraunhofer diffraction) are considered together, it is seen that by their use particle sizes from 10^2 Å to almost 10^7 Å can be investigated. In the remainder of this article, the first two methods will mainly be considered.

1.6. *Salient experimental features*

Since, in the general case, light scattering measurements over a range of angles and concentration are required, the equipment used has mainly been of the type illustrated in figure 5. A light source (usually a Hg discharge lamp with suitable filters or now a He–Ne laser) is used to provide a parallel beam of light which passes into a thermostatic bath (B) surrounding the cell, itself mounted precisely at the centre of rotation of the photomultiplier (PM) detection system. Not only does the bath provide constancy of temperature but it also minimizes reflections at the cell walls and elsewhere. Readings from the photomultiplier system are taken over a range of angles and particularly at the lowest possible angles in view of the subsequent extrapolation. Correction has to be made for the volume viewed and, unless the incident light is plane polarised, by the $(1+\cos^2\theta)$ term. Calibration of the apparatus is conveniently carried out against careful spectrophotometer measurements on strong Rayleigh scattering systems or against secondary standards (see Appendix A).

Several modern commercial versions of the apparatus shown in figure 5, which can also be used for dynamic light scattering, are available (e.g. Malvern, Coulter, Brookhaven, ALV-Langen Co.). A laser replaces the traditional mercury light source and a photon counting multiplier the simple nine-stage photomultiplier, but such equipment is quite suitable for integrated intensity measurements. To achieve very low

scattering angles ($< 15°$) the avoidance of stray light is of considerable importance and devices for achieving this have been described (e.g. Godfrey, Johnson and Stanley (1982)).

A different approach was provided in the Chromatrix (now Milton Roy) KMX-6 Low Angle Laser light scattering apparatus, where the scattered laser light at low angles (in the range 3°–7°) is collected through an annular aperture in an opaque disc placed in the emerging light beam. By utilising the transmitted light also, the ratio of scattered to incident intensity is obtained and with $P(\theta) \approx 1$, absolute molecular weights may be obtained. With low-powered laser optics and special cell, small volumes of liquid only are required and the apparatus is well suited to the examination of the eluate from a chromatographic column. However great care is required in avoiding particulate debris from such columns which would have a preponderant effect at low angles.

More recently the Dawn multi-angle laser light scattering instrument, equipped with an array of 15 photodiode detectors suitably distributed over a broad angular range (5°–175°), has been introduced. This arrangement gives a very complete intensity v angle envelope. With specially designed software, this data at several concentrations can be rapidly used to construct a Zimm plot, thus providing weight-average molecular weights and Z-average radii of gyration. The apparatus can also be used in a 'flow' mode following a chromatographic column with concentration measuring devices (e.g. ultraviolet absorption or refractive index), though the shedding of column material is a potential hazard.

For molecular weights lower than 200 000, the most serious experimental problem lies in providing adequate clarification of the solutions studied. All traces of dust, fibrous impurities, and aggregation products must be removed, usually by repeated ultrafiltration or, if this is not possible, by ultracentrifugation. This requirement has probably been the chief cause of the method falling largely into disuse in the biochemical field over the years 1955–1975. So often, a new carefully fractionated material occurs in such small quantity that the necessary clarification procedures cannot be performed, and optical measurements on incompletely clarified solutions are not useful.

1.7. *Results*

Although integrated light scattering has not been greatly used recently, the method was used earlier to measure or confirm the molecular weights of many well-defined proteins and polymeric materials. Such values have been well tabulated (e.g. Stacey (1956), Tanford (1961)) and need not be repeated here. Suffice it to say that, for well-defined materials, light scattering molecular weights are in general agreement with those obtained by other techniques (particularly sedimentation and diffusion methods). Where doubt occurs, it is usually associated with difficulty in clarifying a solution sufficiently for light scattering requirements. The values range from low molecular weight enzymes ($\sim 10\,000$) to viruses and nucleic acids (10^6–10^8).

Radius of gyration values, obtained normally through equation (11) from Zimm plots of light scattering data, have also been reported for different types of polymeric material. For proteins this is practicable only for the more asymmetric molecules. The muscle protein, myosin, and tobacco mosaic virus with R_g values of 468 Å and 924 Å respectively are typical examples (see Tanford (1961)). Linear synthetic polymers have been much investigated in this way. Thus it has been possible to show the increase in R_g

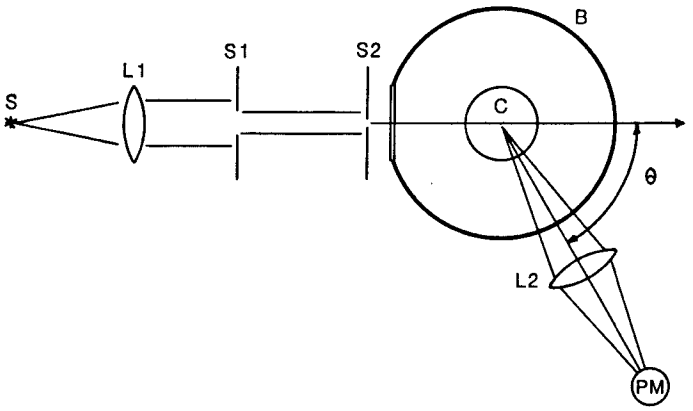

Figure 5. Typical traditional light scattering apparatus, S—light source, S_1, S_2—apertures, L_1, L_2—lenses, B—thermostated bath, C—cell. PM—photomuliplier.

with temperature for such polymers in a poor solvent and from the variation in R_g with molecular weight the stiffness of the chain structure could be assessed. Thus poly-*v*-benzyl-L-glutamate in chloroform-formamide at 25°C was shown to be rodlike (with R_g/M constant) and polystyrene in butanone 22°C was randomly coiled (with $R_g/M^{1/2}$ constant).

2. Properties of laser radiation

The introduction of the laser has led to considerable improvements in classical light scattering techniques but, much more importantly, to fundamental extensions of the method. These have been termed dynamic or quasi-elastic light scattering but the terms intensity fluctuation spectroscopy, and photon correlation spectroscopy are also commonly used. In the remainder of this article, we shall be concerned with these developments, but first it is necessary to deal with the fundamental properties of laser radiation. For this purpose we will consider a continuous wave laser of the helium–neon or argon ion type.

By the nature of the resonating laser cavity, a very obvious property is the 'ready-made' collimation of light which is achieved. Thus a beam divergence of 1 millirad is commonly quoted—this means that at a distance of 1 km. the laser would give an illuminated spot of 1 m diameter. With such collimation the angular resolution attainable in light scattering experiments is clearly superior to that obtained using gas discharge sources of light. Alongside this high degree of collimation, and with the concentration of power into a small area (e.g. 1 mm^2), the intensity achieved in a simple gas laser is commonly four or five orders of magnitude greater than that for conventional sources. As to line width, with measures taken to ensure single mode operation, the frequency spread may be less than 10^3 Hz (or $\Delta\nu/\nu \approx 10^{-13}$), but without such measures many longitudinal (e.g. 10–20) and other modes may be operating so that a spread of about 1600 MHz may occur. Even so this is an order of magnitude better than is normally achieved with conventional sources and filters.

However perhaps the most important property is the high degree of coherence of laser radiation, which arises from the mechanism of light amplification by stimulation of the emission of the radiation. Thus emitted photons are in phase with the exciting photon, and for a plane wave, the phase across any plane perpendicular to the direction

of propagation, is the same. The radiation is said to be spatially coherent. This is a fundamental requirement of the radiation in dynamic light scattering.

A recent development is the use of diode lasers as light sources. With coherence properties somewhat poorer than those of conventional lasers but wavelengths as low as 670 nm, such devices, which are now being actively developed, provide a much smaller and less expensive alternative. To achieve good collimation they require the use of cylindrical lens elements, and, for constancy of wavelength, a constant operating temperature. Undoubtedly diode lasers will eventually replace many of the lower powered conventional lasers now in use.

3. Dynamic light scattering

Ramachandran (1943) described the effect of placing a glass plate, upon which lycopodium powder was dusted, in the path of a light beam passing through it perpendicularly. A pattern of stationary spots was produced, but he suggested that if the scattering particles were to move then the pattern of spots would also change. He reported that Raman had suggested that such an approach could be used for the investigation of the Brownian motion of scattering particles. This suggestion has been completely confirmed by the development of dynamic light scattering. The modern counterpart of Ramachandran's experiment is to direct a laser beam through a polystyrene latex suspension (or a suspension of strongly scattering particles). If the emerging laser beam is allowed to fall upon a plane surface at a distance of 3 or 4 m, a pattern of randomly moving bright spots on a dark background is observed—the so-called 'speckle' pattern. Such a pattern may be thought of in terms of a set of Bragg reflections in which movement is caused by the Brownian movement of the scattering particles. If a small detector is placed on one of the bright speckles, then the intensity would be shown to vary irregularly (e.g. as in figure 6(*a*))—hence the name used frequently of Intensity Fluctuation Spectroscopy. A detailed knowledge of the intensity fluctuations can be used to determine the nature of the motion of the scattering particles, as will be shown below.

An alternative viewpoint is that the motion of the scattering particles imposes Doppler components on the initially sharply monochromatic incident wavelength and since the particles in Brownian motion are moving randomly, there will be a spread of

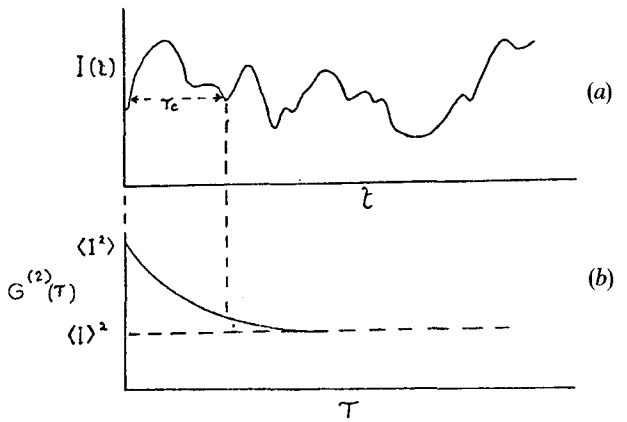

Figure 6. (*a*) Plot of intensity, $I(t)$, at time (t) against time. (*b*) $G^{(2)}(\tau)$ as function of τ for intensity plot (*a*).

wavelength to both higher and lower values. The different wavelengths will, of course, beat amongst themselves giving the intensity fluctuations mentioned above. Spectrum analysers may be used to investigate such effects, and in certain types of work (particlarly electrophoresis) have been used very successfully in conjunction with multi-channel analysis or other recording devices (e.g. see Ware (1982)). However remarkable developments of the correlation method of investigating intensity fluctuations have taken place in the last 15 years. These involve sophisticated digital computing methods, of which a brief outline will be given below. Most applications of dynamic light scattering thus make use of a digital correlator which is merely a purpose-built computer. Such instruments are available commercially (e.g. Malvern Precision Instruments, Spring Lane, Malvern, Worcs., UK, Coulter Electronics Ltd., Luton, UK) and are being developed continuously.

3.1. *Theoretical principles*

Consider an irregularly fluctuating intensity of the type shown in figure 6 (*a*)—$I(t)$ is the intensity at a given time t. The intensity behaviour may be described in terms of the intensity correlation function, $G^{(2)}(\tau)$, defined as

$$G^{(2)}(\tau)=\frac{1}{T}\int_0^T I(t)I(t+\tau)\,\mathrm{d}t=\langle I(t)I(t+\tau)\rangle. \tag{12}$$

Here T must be large and τ small compared with the time required for the intensity to complete a cycle of variations, τ_c. The angled brackets denote averaging over a time long compared to the cycle length.

At very short values of τ, $I(t)\sim I(t+\tau)$, so that $G^{(2)}(\tau)$ approximates the mean value of I^2, whereas at high τ values, there will be no correlation between the I values; thus $G^{(2)}(\tau)$ approximates $\langle I\rangle^2$ as shown in figure 6 (*b*). Variation of $G^{(2)}(\tau)$ occurs mainly over a time τ_c as is to be expected from its definition. It is convenient to normalize the correlation function by dividing by $\langle I\rangle^2$ obtaining

$$g^{(2)}(\tau)=\frac{\langle I(t)I(t+\tau)\rangle}{\langle I\rangle^2}. \tag{13}$$

It can be shown (e.g. see Pusey and Vaughan (1975) that $g^{(2)}(\tau)$ may theoretically be as high as 2, though experimental factors may limit it to lower values: at high τ values $g^{(2)}(\tau)$ approaches unity. The detailed variation of $g^{(2)}(\tau)$ between its extremes depends upon the nature of the scattering system, and it is with the examination and interpretation of such variation that dynamic light scattering is concerned.

In reality, with the usual experimental arrangements, numbers of photons, $n_s(t)$, arriving in a small sample time s centred at time t are measured and the various specialized computers or correlators evaluate the function $\langle n_s(t)n_s(t+\tau)\rangle/\langle n_s\rangle^2$ at 128–256 different values of τ. Though it is not obvious, it can be shown that this function is identical with $g^2(\tau)$ as defined above i.e.

$$g^2(\tau)=\frac{\langle n_s(t)n_s(t+\tau)\rangle}{\langle n_s\rangle^2}. \tag{14}$$

Our concern has been as yet with the intensity correlation function since this is normally measured experimentally, but it is possible to construct a similar function,

$g^1(\tau)$, in terms of the electric field which has theoretical advantages. Fortunately, for random scattering processes, the two correlation functions are simply related:

$$g^1(\tau)=(g^2(\tau)-1)^{1/2}. \tag{15}$$

Thus a determination of $g^{(2)}(\tau)$ also gives $g^{(1)}(\tau)$ which can readily be related to the properties of scattering systems. It can be shown that $g^{(1)}(\tau)$ varies from the value 1 at low τ to zero at long times.

3.2. *The scattering process*

Consider a plane monochromatic wave incident upon a collection of N similar, randomly placed scattering particles (figure 7(*a*)). The process of scattering is conveniently treated in terms of the various wave-vectors. Let the incident wave-vector $\mathbf{k}_i$ for which $|\mathbf{k}_i|=2\pi n/\lambda_0$, and that for the scattered wave $\mathbf{k}_s$ with $|\mathbf{k}_s|=2\pi n/\lambda_0$, λ_0 *being* the wavelength in vacuo, and n the refractive index of the medium. The scattering vector, $\mathbf{K}$, is defined by

$$\mathbf{K}=\mathbf{k}_i-\mathbf{k}_s. \tag{16}$$

From figure 7(*b*)

$$|\mathbf{K}|=2\frac{2\pi n}{\lambda_0}\sin\theta/2=\frac{4\pi n}{\lambda_0}\sin\theta/2. \tag{17}$$

Each particle will scatter light whose amplitude will usually be a function of θ and time, or more generally $A_i(K,t)$, i referring to the particular particle and $K=|\mathbf{K}|$. The factors determining A_i, are those already considered in connection with equations (1)–(3). The phase of each contribution will depend upon the particular position of the particle in question. Let us assume one particle at the point 0 in figure 7(*a*) and another i at the position $\mathbf{r}_i(t)$ relative to 0. Then from optical theory, the phase difference between them is given by the scalar product:

$$\mathbf{K}\cdot\mathbf{r}_i(t). \tag{18}$$

Then the total amplitudes of the light scattered by all the particles is given by

$$E(K,t)\propto\sum_{i=1}^{N}A_i(K,t)\exp[i\mathbf{K}\cdot\mathbf{r}_i(t)]. \tag{19}$$

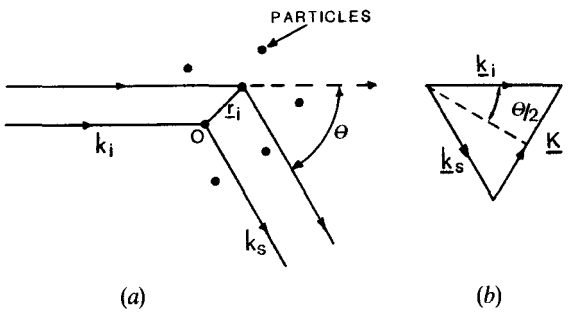

Figure 7. (*a*) Light scattering geometry. (*b*) The relation of wave (**k**) and scattering vectors (**K**).

The numerator of the field autocorrelation function may then be written

$$\langle E(K,0)E^*(K,t)\rangle = \sum_{i=1}^{N}\sum_{j=1}^{N}\langle A_i(K,0)A_j(K,t)\exp\{i\mathbf{K}\cdot[\mathbf{r}_i(0)-\mathbf{r}_j(t)]\}. \tag{20}$$

This expression may appear formidable but for a dilute suspension of small (cf λ) particles or larger spherical particles.

$$A_i(K,0) = A_i(K,t) = \text{constant}.$$

A further simplification occurs on averaging when only those terms for which $i=j$ are retained. Thus the *normalized* field correlation function becomes

$$g^{(1)}(t) = \langle\exp\{i\mathbf{K}\cdot[\mathbf{r}(0)-\mathbf{r}(t)]\}\rangle = \langle\exp[i\mathbf{K}\cdot\Delta\mathbf{r}(t)]\rangle, \tag{21}$$

where $\mathbf{r}(t)$ is the vector displacement of the particle in time t. To obtain the average of the exponential term, we make use of the expression

$$P(r,t/0,0) = \frac{1}{(4\pi Dt)^{3/2}}\exp(-r^2/4Dt), \tag{22}$$

where $P(r,t/0,0)$ is the probability of finding the particles, initially at the origin, at position r after time t, and D is the free particle diffusion coefficient (see Clark, Lunacek and Benedek (1970)). Thus we obtain†

$$g^{(1)}(t) = \exp(-DK^2t), \tag{23}$$

from which we observe that the time required, τ_c, for $g^1(t)$ to fall to $1/e$ times the initial value is

$$\tau_c = \frac{1}{DK^2} = \frac{\lambda^2}{D(4\pi\sin\theta/2)^2}, \tag{24}$$

where λ is the wavelength in the solution. But from kinetic theory (e.g. see Moelwyn-Hughes (1957)), the time required for a particle to diffuse a distance λ is given by $\lambda^2/2D$. Since $4\pi\sin\theta/2$ is of the order of unity, τ_c may be visualized as the time required for diffusion through a distance λ. If $g^{(1)}(t)$ can be evaluated through equation (15), then a plot of $\ln g^{(1)}(t)$ against t should give a straight line with slope $-DK^2$, from which the value of the translational diffusion coefficient can be determined. It should be observed that since K is proportional to $\sin\theta/2$, then for a given D value, the exponential decay of $g^1(t)$ is slower, the lower the angle of observation θ.

3.3. *The effect of polydispersity*

Equation (23) holds only for a dilute homogenous suspension of scattering particles with dimensions much smaller than λ (i.e. Rayleigh scatterers) or somewhat larger particles of spherical shape. Frequently, however, though the particles may approximate Rayleigh scatterers, they may vary considerably in size and correspondingly in diffusion coefficient. In such a situation we expect the larger D values to make the larger contribution at shorter times, so that a plot of $\ln g^1(t)$ against time would show

† τ has already been used as the argument of the field correlation function, $g^{(1)}$. However, in much literature and in the remainder of this article t and τ will be used interchangeably.

curvature (as is commonly observed). In fact, as shown below, if the limiting slope at low t values can be determined it provides the z-average diffusion coefficient defined by

$$D_z = \frac{\sum N_i M_i^2 D_i}{\sum N_i M_i^2}, \tag{25}$$

where N_i is the number of molecules of molecular weight M_i and diffusion coefficient D_i. This average arises from the fact that the scattering intensity from N_i molecules of molecular weight M_i is proportional to $N_i M_i^2$ (see Appendix B). D_z is a useful quantity which when combined with weight-average sedimentation coefficients yields a weight-average molecular weight (as long as the partial specific volume is constant throughout the sample).

If it is assumed that there exists a distribution of diffusion coefficients, we can write

$$g^{(1)}(t) = \int P(D) \exp(-DK^2 t)\, \mathrm{d}D, \tag{26}$$

where $P(D)$ is the distribution of diffusion coefficients weighted by the scattering properties of the different particles. We can also write for the mean diffusion coefficient, $\bar{D}$.

$$\bar{D} = \int DP(D)\, \mathrm{d}D. \tag{27}$$

Pusey (1974) showed by expanding the exponential in equation (26) about $\bar{D}$ that

$$\ln g^{(1)}(t) = -\bar{D}K^2 t + \frac{(\overline{D^2} - \bar{D}^2)}{2} K^4 t^2 + \text{higher terms}. \tag{28}$$

If equation (28) can be fitted to a polynomial in $K^2 t$ and the coefficients obtained, then the coefficient of the first two terms gives $(\overline{D^2} - \bar{D}^2)/\bar{D}^2$, i.e. the z-averaged normalized variance of the distribution of diffusion coefficients (later termed polydispersity factor (PF)). As would be expected, the quantity thus determined is of lower accuracy ($\pm 0{\cdot}02$ at best) than the diffusion coefficient (± 2–5%) but particularly for the narrower distributions, it gives a useful measure of the distribution. Thus Pusey (1974) has shown that it can be related to other measures of polydispersity e.g. M_z/M_w and M_W/M_N, the subscripts N, W, Z indicating number, weight and Z averages. Experimental limitations prevent the useful utilization of the higher terms of equation (28).

3.4. *Asymmetric and flexible particles*

It was pointed out following equation (20) that for small particles and larger spheres, the scattering amplitude term was a constant, independent of angular position or time. However when the scattering particles become comparable in dimensions with wavelength (e.g. $> \lambda/20$) and deviate from spherical symmetry, then the scattering amplitude becomes a function of time i.e. $A_i(K, t)$. This means that as a rigid particle rotates or a linear polymer vibrates, the intensity of scattering fluctuates, and this effect is additional to that already considered arising from the translational motion of the particle.

For the rotation of rigid rod-like particles, the expression for $g^1(t)$ becomes

$$g^{(1)}(t) = A_0(K) \exp(-DK^2 t) + A_1(K) \times \exp[-(DK^2 + 6D_R)t] + \text{other terms} \tag{29}$$

where A_0 and A_1 are K-dependent amplitudes, and D_R is the rotational diffusion coefficient. Simplification results when the angle of observation is reduced to the lowest possible value (e.g. $<5°$). Under such conditions, (i.e. where $A_0 \gg A_1$) the contribution of the rotational motion may be reduced to such a low level that only the effects of translational motion are observed (see Berne and Pecora (1976)).

For flexible linear polymers in dilute solution. Pecora (1965) laid the foundations of dynamic light scattering in terms of the normal modes of vibration. Thus $g^1(t)$ may be expressed as

$$g^1(t)=\exp(-DK^2t)[P_0+P_{21}\exp(-2t/\tau_1)+P_{12} \times \exp(-t/\tau_2)+P_{22}\exp(-2t/\tau_2)+P_4\exp -4t/\tau)+\ldots], \quad (30)$$

where τ_1 and τ_2 are the relaxation times of the first two normal modes and the relative amplitudes of these terms, (as for equation (29)) depend strongly on the parameter $x=K^2\langle R_g\rangle^2$, R_g being the radius of gyration of the polymer. For values of $x>7$, terms in addition to those in equation (30), are required. Relaxation times may be expressed in terms of other polymer properties. Thus for non-draining chains (Zimm model)

$$\tau_1=0{\cdot}847M\eta_s[\eta]/RT, \quad (31\,a)$$

or

$$\tau_1=5{\cdot}84\eta_sR_g^3/kT, \quad (31\,b)$$

where M and $[\eta]$ are the molecular weight, and intrinsic viscosity, η_s being the viscosity of the solvent, R and k being the gas constant and Boltzmann constant. Higher mode (p) relaxation times for this model are given by

$$\tau_p=\tau_1/p^{1\cdot5}. \quad (32)$$

Relaxation time values obtained from equation (30) and similar equations may be compared with those calculated from equations (31) and (32) as well as from different models. This is however only profitable if $g^1(t)$ can be obtained over a large range of t values. Examples of such systems are provided under Results.

3.5. *Scattering by motile micro-organisms*

As yet, we have considered only those particle displacements which are caused by Brownian motion. If we turn to micro-organisms, then in addition to Brownian motion, we must consider the effects of their own motility which in many cases are much the greater. Equation (21) is still applicable to the effects of motility, but the displacement must now be written in terms of the motion of the organism. Where the velocity is constant over a distance long compared with K^{-1} (an effective wavelength or repeat distance for the experiment), then $[\mathbf{r}(0)-\mathbf{r}(t)]$ may be replaced by $\mathbf{V}t$ where $\mathbf{V}$ is the swimming speed. Then

$$g^{(1)}(t)=\int_0^\infty \exp(i\mathbf{K}\cdot\mathbf{V}t)p(\mathbf{V})d^3\mathbf{V}, \quad (33)$$

where $P(\mathbf{V})$ is the velocity distribution for the organism and the integration is performed over all values of $\mathbf{V}$. If the velocity distribution is completely isotropic, then equation (33) simplifies to

$$g^{(1)}(t)=\int_0^\infty \frac{\sin K\mathbf{V}t}{K\mathbf{V}t}P(\mathbf{V})\,d\mathbf{V}. \quad (34)$$

Under some circumstances this equation may be inverted to give $P(\mathbf{V})$ but more usually a single-parameter speed distribution is assumed (see Chen and Hallett (1982)) e.g. a Maxwellian distribution. Curve fitting on a computer can then give the distribution parameter and the complete velocity distribution. Normally, however, it is necessary to make allowance for a fraction of non-motile organisms which are undergoing only Brownian motion. A satisfactory curve-fitting computer programme will then give the fraction of motile organisms, the velocity distribution and its various derived properties, as well as the Brownian diffusion coefficient of the non-motile fraction (figures 17–19).

However the assumption of isotropic velocity distribution cannot be be generally made. In many situations motion may be in a specific direction, straight-line motion may be interrupted by 'twiddles', and in other cases a spiral type of motion occurs. The study of all these complications has begun but space forbids its treatment here. A general point, however, should be made. When the particle is comparable in dimensions with λ, is asymmetric and has a non-uniform refractive index, it may be necessary to combine measurements of intensity v angle with dynamic measurements. By comparing calculated intensity v angle curves with those computed from mathematical modelling, detailed optical properties may be derived which then allow a fuller treatment of the dynamic light scattering data (see Chen and Hallett (1982)). This however is a complex field in which Mie (1908) theory for spheres requires extension to the various particle shapes encountered.

3.6. *Application of the method*

In many features, the optical components of figure 8 are similar to those of figure 5. A coherent laser beam (15–100 mw) falls upon a small volume (1–2 ml) of the scattering suspension contained in a cell, carefully positioned in a thermostated water bath, provided with a plane entrance window and a cylindrical, good quality polycarbonate (or other transparent) exit window. The light scattered by a very small volume (0·05 ml) at a given angle (θ) is collected by a carefully positioned slit system (possibly accompanied by a lens) and received on the small sensitive surface of a photon-counting photomultiplier tube (PM) (e.g. EMI 9863). With a fast recording device, it

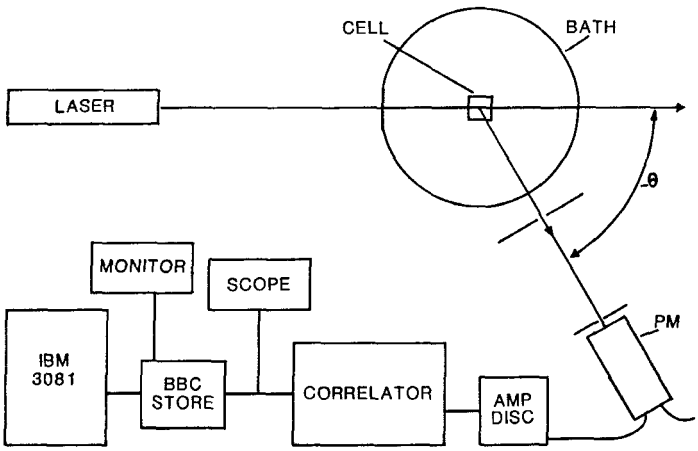

Figure 8. Apparatus for dynamic light scattering.

would be possible to observe irregular fluctuations in the scattering intensity comparable with those at a spot in the 'speckle' pattern mentioned earlier, but usually the signal from the photomultiplier proceeds to an amplifier–discriminator by which the output pulses are shaped (to 30 ns width) and given appropriate amplitude (−2 V). These then proceed to the correlator, a purpose-built digital computer whose function it is to calculate the correlation function as defined by equation (13). For this purpose the correlator sets the duration of the experiment, the sample time, τ, (from $10^{-8} = 10^{-3}$ s), counts the total number of samples, the total number of pulses, and calculates the product in the numerator of equation (14) for 128–256 values of the time delay, each a multiple of the sample time. The very large numbers are retained in various registers of the correlator and the progress of the experiment can be seen on an oscilloscope where the correlation products as a function of time are displayed. After a time, which may vary from a few seconds for strongly scattering systems (e.g. micro-organisms) to 30 min for weakly scattering solutions of low molecular weight enzymes, the experiment is terminated. The output from the correlator is stored in a BBC or similar micro-computer and eventually transferred to a main frame computer (e.g. the IBM 3081) for calculation of normalized $g^{(2)}(t)$ values, for plotting $\ln(g^{(2)}(t)-1)$ against time, and determination of diffusion coefficients, variance of diffusion coefficients or other desirable features. In the most recent versions of the apparatus, signals from the photomultiplier are directed to a correlator–microcomputer combination equipped with suitable software so that the above computations (or alternatives) are produced 'on line'.

Unless the scattering is very strong, it is necessary to ultra-filter solutions repeatedly to remove extraneous strongly scattering material. In this respect, dynamic light scattering does not differ from the classical version. However because the scattering volume is so small, it is possible to work with somewhat smaller volumes of clarified solution (e.g. 0·5 ml), though the author has reservations about the the use of capillary type cells owing to the optical distortions inevitably occurring then.

3.7. *Typical results*

Dynamic light scattering has been applied to numerous systems for the determination of translational diffusion coefficients. Figure 9, a copy of the computer output for turnip yellow mosaic virus (TYMV), demonstrates the great precision of the data (see also Godfrey, Johnson and Stanley (1982)). Diffusion coefficients accurate to $\pm 0{\cdot}2\%$ are obtainable for such strongly scattering systems. Further, figure 10 shows the constancy of the measured values over a large angular range, and figure 11 the variation of measured D values with concentration for different solution conditions. Similar sedimentation coefficient (S°_{20}) data was also obtained. Using $D^\circ_{20} = 1{\cdot}425 \times 10^{-7}\,\mathrm{cm^2\,s^{-1}}$, and $S^\circ_{20} = 114{\cdot}0$ Svedbergs, with a partial specific volume of 0·661, a molecular weight of $5{\cdot}73 \times 10^6$ was obtained. For well-filtered TYMV preparations, the PF value achieved values as low as 0·025 but less clarified solutions gave much higher values (even >1).

As an example of lower molecular weight solutes, figure 12 contains a plot of $\ln[g^{(2)}(\tau)-1]$ against channel number (i.e. τ divided by sample time) for an enzyme, HMG Co-A Synthase (molecular weight = 96 000) in which the precision of the data is clearly lower. At the other end of the range, figure 13 contains a plot of $\ln[g^2(\tau)-1]$ against number for tobacco mosaic virus (TMV—of molecular weight 42×10^6) for $\theta = 15°$ in phosphate buffer ($I = 0{\cdot}0125$) at pH 7·5 and 25°C (Johnson and Brown 1992.

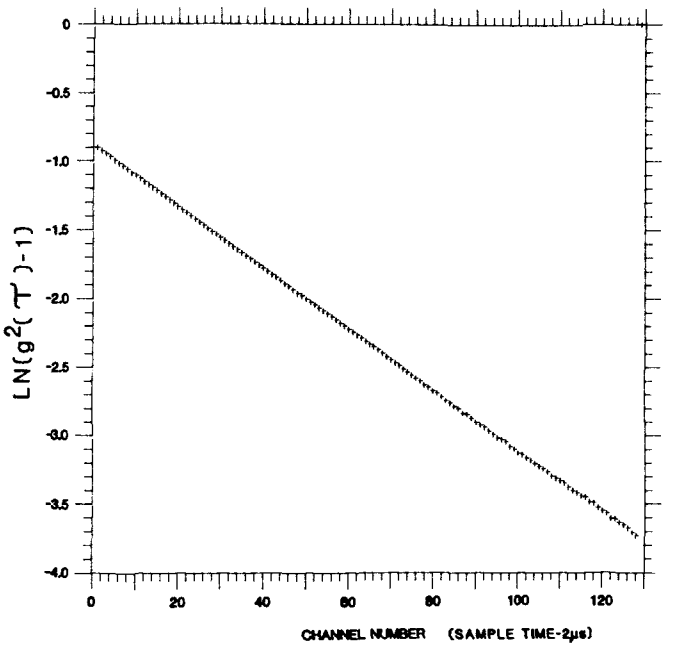

Figure 9. Plot of $\ln[g^2(\tau)-1]$ against channel number for TYMW at a concentration of 0·32 g(100 ml)$^{-1}$ under neutral conditions. Sample time $-2\,\mu s$.

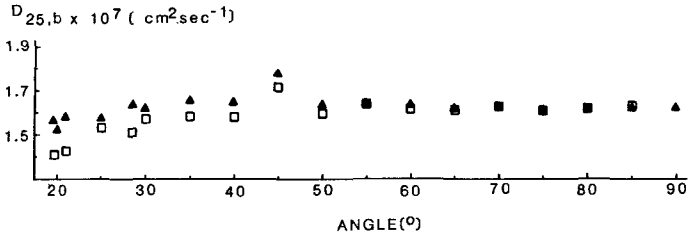

Figure 10. Plot of diffusion coefficient, $D_{25,b}$, for TYMW at 25° in phosphate buffer (pH 6·5) against angle θ. □—sample time, 3 μs. ▲—sample time modified by factor $(\sin 45°/\sin \theta/2)^2$.

For this angle, only the first term of equation (29) is required so that the slope of the line gives the translational diffusion coefficient (D) directly. At higher angles both terms are required and by suitable curve fitting procedures assuming D from lower angles, the rotational diffusion coefficient, D_R, could also be obtained. To achieve even modest accuracy (e.g. ±5%) in this, it was necessary to ensure that the coefficient $A_1(K)$ was an appreciable fraction of $A_0(K)$ by using as high a θ value as possible. Figure 14 contains a plot of $g^1(\tau)$ against channel number for TMV at 90° and under solution conditions similar to those of figure 13 where experimental points as well as the fitted curve are shown. The translational diffusion coefficients, accurate to ±0·5%, were found to decrease slowly with increasing TMV concentration but the much less precise D_R values (±5%) showed no detectable concentration effect.

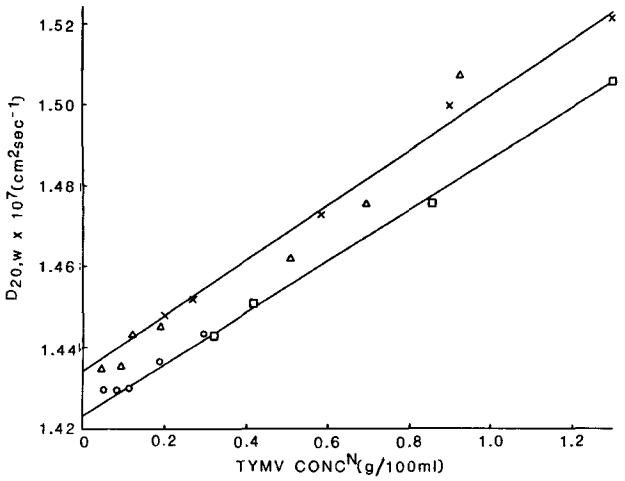

Figure 11. Plot of corrected diffusion coefficient ($D_{20,w}$) against TYMV concentration Δ, $x-0{\cdot}1$ M Acetate at pH 5·4: ○—Phosphate–NaCl ($I=0{\cdot}1$) at pH 6·8: □-Phosphate–NaCl ($I=0{\cdot}24$) at pH 7·3.

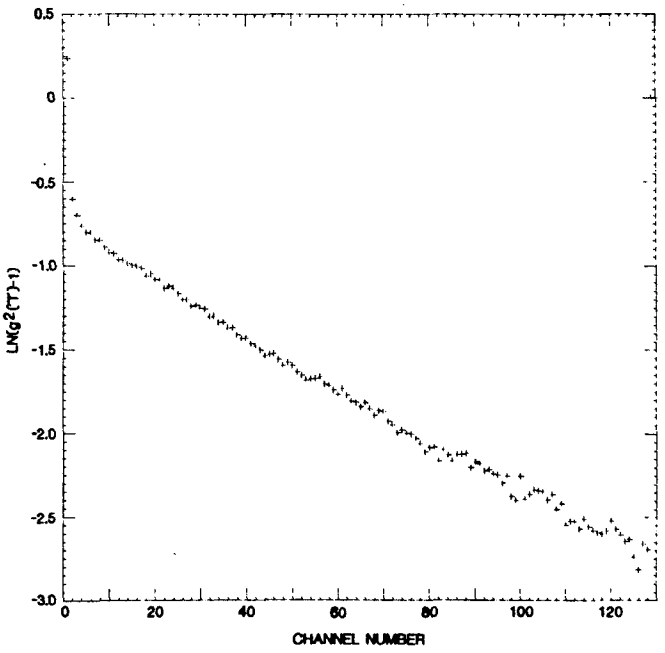

Figure 12. Plot of $\ln[g^2(\tau)-1]$ against Channel number for HMG CO-A Synthase ($0{\cdot}78$ g$(100\,\text{ml})^{-1}$) in Phosphate–NaCl buffer at $I=0{\cdot}1$, pH $=7{\cdot}0$. Sample Time—$0{\cdot}5$ μs.

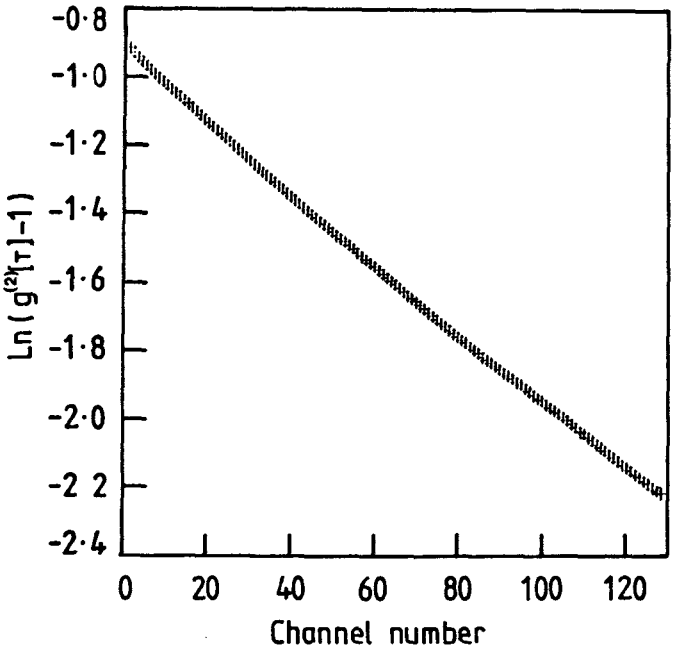

Figure 13. Plot of $\ln(g^2(\tau)-1)$ against channel number at 25° for TMV (0·119 g(100 ml)$^{-1}$) in phosphate buffer at $I=0{\cdot}0125$, pH 7·5. $\theta=15°$. Sample Time = 100 μs.

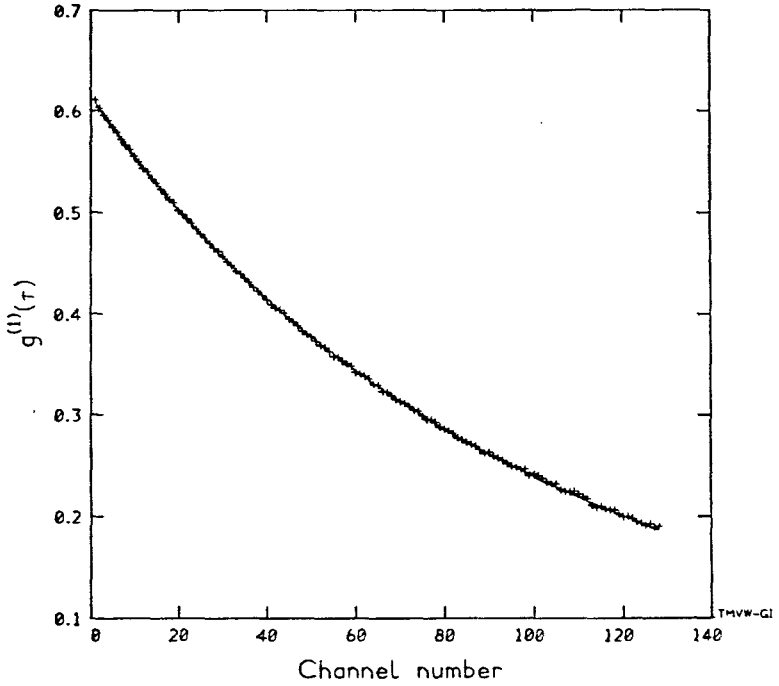

Figure 14. Plot of $g^1(\tau)$ against channel number for TMV (0·067 g(100 ml)$^{-1}$) in phosphate buffer at $I=0{\cdot}0125$, pH 7·5 at 25°C. $\theta=90°$. Sample time = 5 μs + exptl points. Full line-computed curve with $D=4{\cdot}70\,\text{cm}^2\,\text{s}^{-1}$ and $D_R=324\,\text{s}^{-1}$.

Investigating the internal dynamics of long chain flexible molecules in solution is a much more difficult problem. From equation (30) it is clear that many unknown quantities are to be evaluated and, as in the case of TMV, a beginning usually involves the evaluation of the translational diffusion coefficient, usually at low angles. Nicolai, Brown and Johnsen (1989) investigated high molecular weight polystyrenes in both cyclohexane at the theta temperature (34·5°C) as well as in toluene and using a variety of sophisticated data handling techniques (including maximum entropy analysis and Contin) were able to estimate the relaxation time (τ_1) of the first internal mode. Difficulties in achieving accuracy are due to the small contribution of the internal modes at low x values, whereas at higher x, the methods available do not resolve the various modes. The value obtained was significantly lower than calculated from the polymer parameters for the non free-draining model of Gaussian chains, but in reasonable agreement with that obtained by other workers for similar material. The calculated value for the free-draining model was even higher and this model was not thought applicable. The authors concede that concentration effects on relaxation times have as yet been ignored but consider such effects will be small at the concentrations used ($\sim 10^{-4}$ g ml^{-1}). Much further work is proceeding along these lines.

A further useful application of dynamic light scattering is to dilute suspensions of micro-organisms. Figure 15 contains a plot of $g^{(2)}(\tau)$ against channel number at $\theta = 90°$ for a suspension of spores of Bacillus Subtilis (Harding and Johnson 1984). Such spores, of dimensions 1·4 × 0·6 μ, scatter very strongly and a curve comparable with figure 15 could be obtained in 50 s. Particles with dimensions greater than the incident wavelength cannot be treated as Rayleigh scatterers and this was confirmed when decay curves obtained over a range of angles showed new features. At low angles, part of the curve, at short times, assumed opposite curvature (see figure 17) and further work is required for its explanation. In the meantime, D values obtained at 90° should be regarded as relative only. Such a D value at 35°C in 0·018 M KCl–0·020 M Tris buffer at pH 8·2 was $5{\cdot}0 \times 10^{-9}$ cm^2 s^{-1}. The Stokes radius derived from this value was 6300 Å, which fits qualitatively the known spore dimensions. The polydispersity factor, PF,

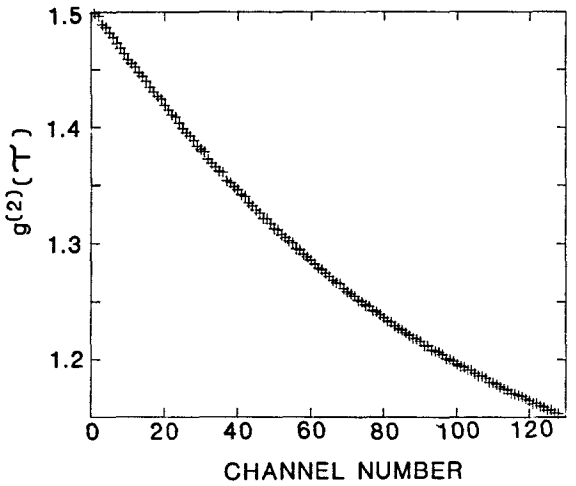

Figure 15. Computer plot for $\theta = 90°$ of $g^2(\tau)$ against channel number for dilute (5×10^7 particles ml^{-1}) suspension of spores of Bacillus Subtilis in 0·018 MKCl–0·020 M Tris (pH 8·2). Sample time – 25 μs. Temperature – 35·0°C.

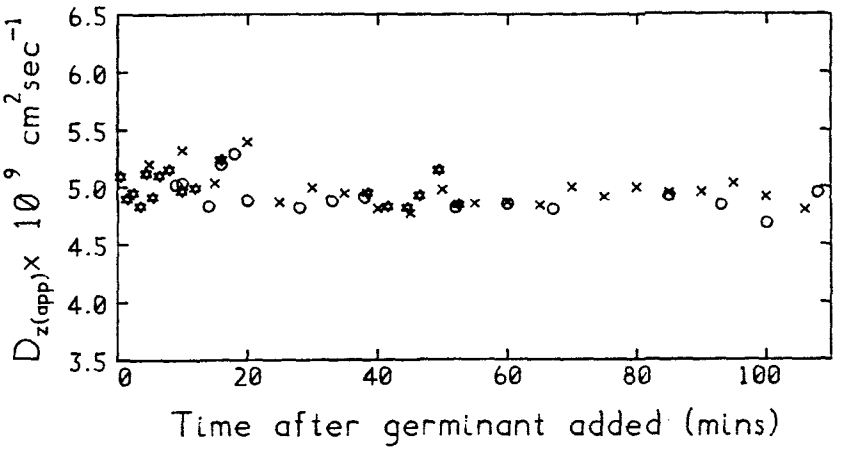

Figure 16. Plot of apparent D_z value against time after addition of 0·02 M 1-alanine as germinant (different symbols denote repeated measurements).

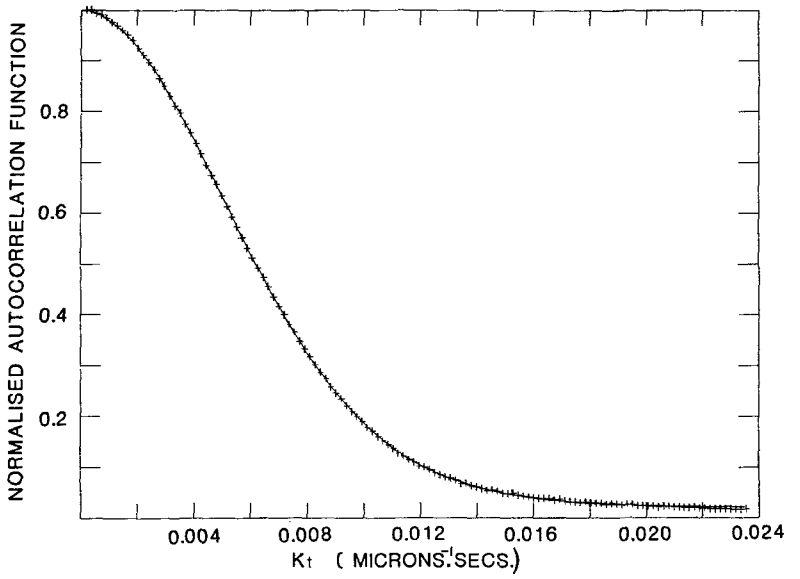

Figure 17. Plot of $g^1(\tau)$ against Kt(microns^{-1} s) for dilute (10^7 particles ml^{-1}) suspension of *Trypanosoma brucei* in Phosphate-buffered glucose containing 0·15% bovine serum albumin at 35°C. Sample time = 40 μs. $\theta = 20°$.

took on values of $0{\cdot}10 \pm 0{\cdot}05$ suggesting inhomogeneity probably due to aggregation. On addition of 0·02 M l-alanine, such a spore suspension germinates and in figure 16, possible changes in the apparent D_z, D_z (app), values were investigated. Clearly no appreciable change occurs which would appear to exclude volume changes.

A final example illustrates the effect of motility on correlation decay curves. The organism involved was *Trypanosoma brucei brucei*, an irregular-shaped thread-like organism of length 15–30 μ and thickness 1·5–2·5 μ, responsible for sleeping sickness in cattle in Africa. The motility of the organism, which can be seen by the optical

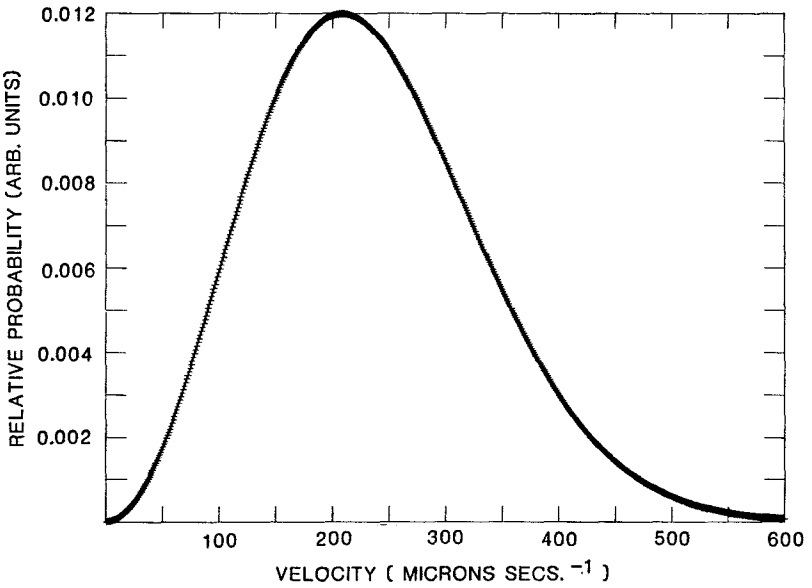

Figure 18. Velocity distribution derived by the computer fit to data of figure 17.

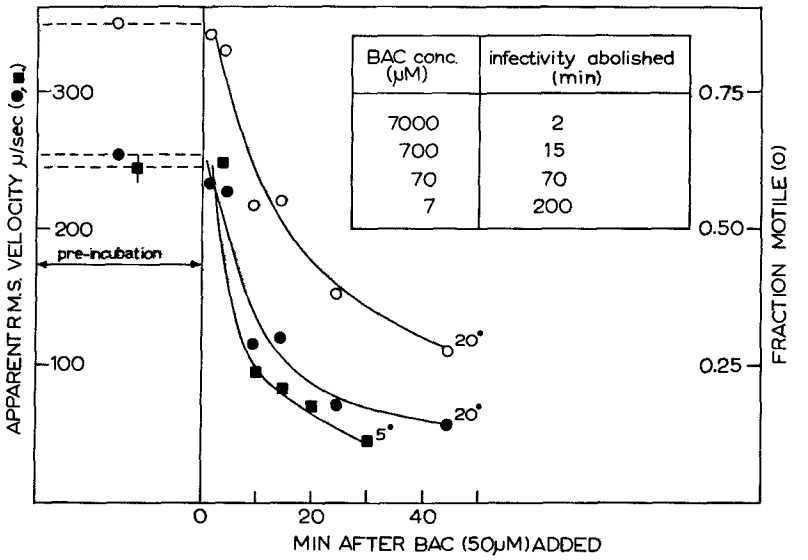

Figure 19. Plots of apparent r.m.s. velocity (●, ■) and motile fraction (○) after addition of 50 M Bromoacetyl-L-carnitine. Temperature −35°C.

microscope, has a profound effect on correlation decay curves. Thus a pronounced Gaussian-type section occurs at low channel numbers followed by an exponential decay of the more usual kind. Figure 17 contains such a correlation decay plot for 35°C and $\theta = 20°$, the continuous line passing through the experimental points (+) being that for the computer fit. The derived velocity distribution is shown in figure 18 for which the apparent r.m.s. velocity was 254 μs^{-1}. In view of the possible complications arising from the shape of the organism and details of the motion, the velocity quoted may have only relative value, but the usefulness of such data is shown in figure 19 (which shows the effect of a drug, bromoacetyl-L-carnitine (BAC) on both apparent r.m.s. velocity and fraction of motile organisms (see Gilbert, Klein and Johnson (1983)). Infectivity data is presented in the table inset. At 50 mM BAC concentration, infectivity would seem to be abolished at about 100 min, by which time, the apparent velocity and fraction of motile organisms have fallen to a low level.

Much more work is required in all the directions mentioned above.

Acknowledgments

I am grateful to my colleagues and co-workers for their cooperation, particularly to Dr S. E. Harding, and to Mr Neville Buttress for his continued experimental assistance. I am also indebted to Professor Sir Sam Edwards for the privilege of working in his department.

Appendix A

Calibration of light scattering instruments

Much thought has been directed to this problem (e.g. see Stacey (1956), Hughes, Johnson and Ottewill (1958), Utiyama (1972)) and no universally agreed method has emerged. $i\theta r^2/I_0$ is of the order of 10^{-4} to 10^{-6} and r is not readily measurable to desired accuracy, so that indirect methods have been devised. In addition to the, now, rarely used procedure of absolute calibration using magnesium oxide (and other) diffusors introduced by Brice, Halwer and Speiser (1950) two groups of methods are used:

(1) The use of highly purified organic liquids (benzene, toluene, carbon disulphide, carbon tetrachloride) whose Rayleigh ratio has been accurately determined by specialized absolute methods (e.g. Coumou (1960), Pike, Pomeroy and Vaughan (1975)). This value would be assumed by workers in the field of light scattering who would purify their own sample of liquid and seal into a cell of high optical quality. The scattering of such liquids is normally of a much lower order than from polymeric or colloidal solutions, and the assumption of identity of scattering for two different samples of a given liquid is not completely satisfactory.

(2) The use of a strongly scattering (often colloidal) but Rayleigh-type solution for which a definite relation between turbidity (or optical density) and R_{90} value may be assumed. The magnitude of the scattering can be adjusted to be similar to that of the solutions to be meausured. Optical density (O.D.) is obtained in a spectrophotometer accurate at low O.D. values and in which low angle scattered light is excluded by restricting apertures. This approach is self-contained in one laboratory and can be repeatedly performed. Uniform polystyrene latex particles in dilute suspension have been used satisfactorily in the author's laboratory.

Appendix B

Averages in light scatterings

$N_iM_i^2$ is effectively the weighting factor in light scattering experiments for molecules of molecular weight M_i. Referring to equation (3), the relevant factor for gaseous systems is $(n-1)^2/v$ which for solution systems becomes $(n-n_0)^2/v$ or $(\Delta n)^2/v$. But since $\Delta n \propto c$ for a given type of polymer and $c_i = v_iM_i/N_0$, the factor is proportional to $v_iM_i^2$ or $N_iM_i^2$. It should, however, be noted that the radius of gyration, R_g, is obtained as a Z average.

References

ADEN, and KERKER, 1951, *J. appl. Phys.*, **22,** 1242.

BENOIT, HOLTZER, and DOTY, 1954, *J. phys. Chem.*, **58,** 635.

BERNE, and PECORA, 1976, *Dynamic Light Scattering* (New York: Wiley).

BRICE, HALWER, and SPEISER, 1950, *J. opt. Soc. Am.*, **40,** 768.

BRUNSTING, and MULLANEY, 1972, *Appl. Optics*, **11,** 675.

CABANNES, 1915, *Compt. Rend.*, **160,** 62.

CHEN, and HALLETT, 1982, *Quart. Rev. Biophys.*, **15,** 131.

CLARK, LUNACEK, and BENEDEK, 1970, *Am. J. Phys.*, **38,** 575.

COUMOU, 1960, *J. Coll. Sci.*, **15,** 408.

DEBYE, 1909, *Ann. Phys.*, (4), **30,** 57; 1915, *Ibid.*, **46,** 809; 1947, *J. phys. Coll. Chem.*, **51,** 18.

DOTY and EDSALL, 1951, *Adv. Protein Chem.*, **6,** 35.

EINSTEIN, 1910, *Ann. Physik*, **33,** 1275.

GILBERT, KLEIN, and JOHNSON, 1983, *Biochem. Pharmac.*, **32,** 3447.

GODFREY, JOHNSON, and STANLEY, 1982, *Biomedical Applications of Laser Light Scattering*, edited by Satelle, Lee and Ware (Amsterdam: Elsevier), p. 373.

HARDING, and JOHNSON, 1984, *Biochem. J.*, **220,** 117.

HECHT, 1987, *Optics*, second edition (Addison-Wesley), p. 396.

HUGHES, JOHNSON, and OTTEWILL, 1956, *J. Coll. Sci.*, **11,** 340.

JOHNSON, and BROWN, 1992, *Laser Light Scattering in Biochemistry*, Royal Soc. Chem., Cambridge, U.K., chap. 11.

KERKER, 1969, *The Scattering of Light* (New York: Academic), p. 54.

LORENZ, 1898, *Ouevres Scientifique* Copenhagen, vol. I, 301, 405.

MIE, 1908, *Ann. Phys.*, **25,** 377.

MOELWYN-HUGHES, 1957, *Physical Chemistry* (London: Pergamon Press), p. 16.

NICOLAI, BROWN, and JOHNSEN, 1989, *Macromolecules*, **22,** 2795.

PANGONIS, and HELLER, 1960, *Angular Scattering Functions for Spherical Particles*, Wayne State University Press, Detroit.

PECORA, 1965, *J. chem. Phys.*, **43,** 1562.

PIKE, POMEROY, and VAUGHAN, 1975, *J. chem. Phys.*, **62,** 3188.

PUSEY, 1974, *Photon Correlation and Light Beating Spectroscopy*, edited by Cummins and Pike (New York: Plenum), p. 387.

PUSEY, and VAUGHAN, 1978, *Dielectric and Relaxation Processes*, edited by M. Davies, (Chemical Society), p. 48.

RAMACHANDRAN, 1943, *Proc. Ind. Acad. Sci.*, A, **18,** 190.

RAMAN, and RAMANATHAN, 1923*a*, *Phil. Mag.*, **45,** 113; 1923*b*, *Ibid.*, **45,** 213.

RAYLEIGH (Third Baron), 1871, *Phil. Mag.*, **41,** 447; 1881, *Ibid.*, **12,** 81.

RAYLEIGH (Fourth Baron), 1918, *Proc. R. Soc.*, **94,** 453.

SMOLUCHOWSKI, 1908, *Ann. Phys.*, **25,** 205.

STACEY, 1956, *Light Scattering in Physical Chemistry* (1977 Butterworths).

SWITHINBANK, BEER, TAYLOR, and MCCREATH, 1977, *Prog. Astronaut and Aeronaut.*, **53,** 421.

TANFORD, 1961, *Physical Chemistry of Macromolecules* (New York: Wiley), p. 307.

UTIMAYA, 1972, *Light Scattering from Polymer Solutions*, edited by Huglin (New York. Academic), p. 61.

VAN DE HULST, 1957, *Light Scattering by Small Particles* (New York: Dover).

WARE, 1982, *Biomedical Application of Laser Light Scattering*, edited by Satelle, Lee, and Ware (Amsterdam: Elsevier), p. 293.

ZIMM, 1948, *J. chem. Phys.*, **16,** 1093.